Energy transfer to erbium ions from wide-band-gap SnO_2 nanocrystals in silica

S. Brovelli,* A. Chiodini, A. Lauria, F. Meinardi, and A. Paleari
Dipartimento di Scienza dei Materiali, Università di Milano-Bicocca, via Cozzi 53, I-20125 Milano, Italy
(Received 22 November 2005; published 28 February 2006)

We give the spectroscopic evidence of energy transfer to erbium ions provided by SnO_2 nanocrystals in silica. The spectral and time resolved analysis of the nanocluster luminescence resonant with Er^{3+} transitions demonstrates that erbium ions take part to energy-transfer mechanisms with an efficiency of about 20%. The spectral features of erbium emission excited by energy transfer allow to ascribe it to Er^{3+} sites in ordered environments, nearby crystalline tin-dioxide nanoclusters.

DOI: 10.1103/PhysRevB.73.073406 PACS number(s): 81.07.Bc, 78.55.Qr, 81.05.Pj

In the last past years, few studies[1–3] demonstrated that energy-transfer mechanisms can occur from silicon quantum dots to erbium ions in silica. Starting from this result, semiconductor nanoparticles in Er-doped silica were proposed as a breakthrough in the attempt of implementing silica-based erbium lasers in integrated optics.[4,5] Indeed, energy transfer from semiconductor nanoclusters to erbium ions can efficiently compensate the small cross section of rare earth transitions,[6,7] providing a realistic perspective of size reduction of Er amplifiers. The possible extension of this result to wide-band-gap nanophases may be interesting because it can confirm and clarify the models proposed to explain the process, and it can also suggest improvements in specific applications. For instance, silica networks with wide-band-gap nanophases are expected to take advantage, with respect to glasses with narrow-band-gap nanoclusters, from the relatively small difference of refractive index of the two phases, with a relevant reduction of transmission losses by Mie scattering.

In this framework, tin-dioxide nanoparticles appear interesting for several reasons: (i) the optical gap lies in the range 3.5–4.5 eV;[8] (ii) the chemistry of tin dioxide permit to grow nanocrystals in silica in a controlled way;[9,10] (iii) SnO_2 nanoclusters makes silica photosensitive and suitable to design an integrated device;[11,12] (iv) rare earth doping in nanostructured SnO_2:SiO_2 can be carried out up to a few mol % without segregation.[13–15] In this work we demonstrate and quantify the occurrence of energy-transfer pathways between excited SnO_2 nanostructures and Er^{3+} ions.

Samples of Er-doped silica with SnO_2 nanoclusters were prepared by a sol-gel technique, with 8 mol % of SnO_2 and 1 mol % Er, by co-gelling tetraethoxysilane, dibutyl tin diacetate and erbium nitrate. After gelation and drying, xerogel samples were heated (about 3 °C/h) in oxygen up to 1050 °C (Ref. 9) to induce SnO_2 nanoclustering and silica densification. Optical grade bulk samples about 1 mm thick were finally obtained. Nanostructure morphology were analyzed by means of transmission electron microscopy (TEM). TEM image in Fig. 1 shows nanoclusters about 4–6 nm in size homogeneously dispersed in the amorphous silica matrix. High resolution images (see inset in Fig. 1) evidence single domain features.

Figure 2(a) shows the optical absorption spectrum of the nanostructured material, collected by means of a spectrophotometer with a spectral bandwidth of 1 nm. The narrow lines correspond to electronic transitions of Er^{3+} ions from the ground state $^4I_{15/2}$ to the indicated excited manifolds. Band-to-band transitions of the SnO_2 nanophase are instead responsible for the absorption edge at about 3.6 eV.[9,11] Photoluminescence (PL) signals were detected by a CCD camera coupled with a polychromator with 1.5 nm bandwidth, and by an InGaS photodiode in the IR range coupled with a monochromator (5 nm bandwidth). PL-excitation (PLE) spectra were obtained by collecting PL at different excitation energies, exciting with a Xe lamp through a monochromator with 5 nm bandwidth. All measurements were corrected for the overall setup spectral response. Time resolved data in the ns time domain were obtained by exciting with the second harmonic of a tunable Ti:Sapphire laser. In the inset of Fig. 2, the absorption spectrum and the PLE spectrum of the 2.25 eV emission are compared. A broad excitation band at 3.6 eV arises from the low-energy tail of the absorption edge of SnO_2.

The PL spectrum [Fig. 2(b), curve *A*] excited within the region of the SnO_2 band-to-band transitions, specifically at 3.70 eV where no intracenter Er^{3+} transition is found, shows two kinds of components: a broad unstructured band centered at 2.1 eV (curve *B*) ascribable to SnO_2 defect states,[8] and a series of positive and negative narrow components (curve *C*) at the energies of the erbium transitions. The Er^{3+}

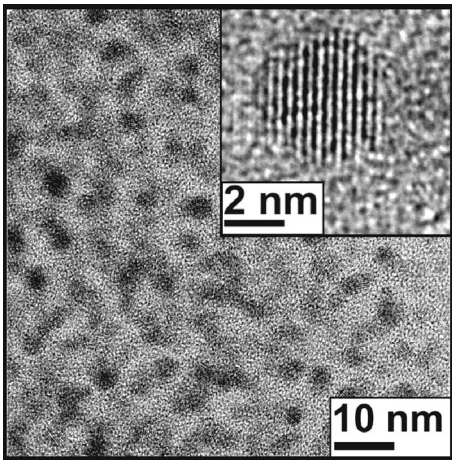

FIG. 1. TEM image of nanostructured 1 mol % Er, 8 mol % SnO_2:SiO_2. Inset, high resolution image of a SnO_2 nanocrystal.

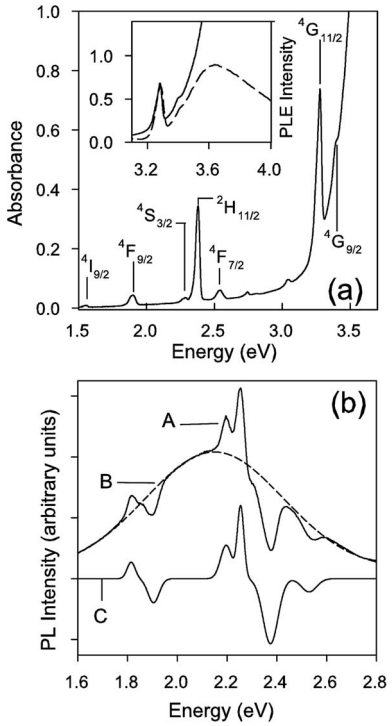

FIG. 2. (a) Optical absorption spectrum of 1 mol % Er, 8 mol % SnO_2:SiO_2. The main Er^{3+} transitions are labeled. Inset, absorption and PLE spectra at $E_{em} \approx 2.25$ eV around the absorption edge of SnO_2. (b) PL spectrum excited at 3.70 eV (curve *A*), Gaussian fit of the broad component (curve *B*), and Gaussian fit of the difference spectrum (curve *C*).

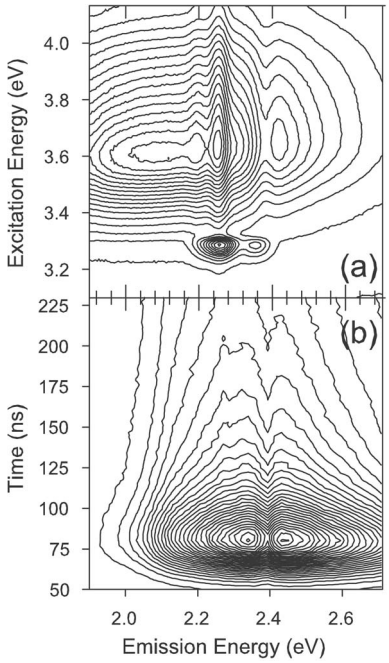

FIG. 3. (a) Contour plot of PL intensity vs excitation and emission energy of 1 mol % Er, 8 mol % SnO_2:SiO_2. (b) Contour plot of PL time decay vs emission energy, exciting at 3.70 eV.

emission at 2.25 eV, due to the $^4S_{3/2} \rightarrow {}^4I_{15/2}$ transition, is structured into two narrow lines. At 2.38 eV, the $^4I_{15/2} \rightarrow {}^2H_{11/2}$ transition gives rise to a strong negative component, i.e., an intensity lowering of the nanophase PL. Other negative components are found at 1.90 and 2.54 eV arising from the Er^{3+} transitions $^4I_{15/2} \rightarrow {}^4F_{9/2}$ and $^4I_{15/2} \rightarrow {}^4F_{7/2}$.

The PL-PLE pattern in Fig. 3(a) clarifies the extension of the resonance region: the broad emission band that dominates the three-dimensional (3D) spectrum is excited within the SnO_2 absorption edge at about 3.6 eV. This PLE band also excites the narrow and structured 2.25 eV emission of erbium. Another evident feature is the excitation-independent lowering of PL intensity at 2.38 [vertical structure in Fig. 3(a)], ascribable to material self-absorption and/or energy transfer processes. In Fig. 3(b) the time decay of PL excited at 3.70 eV is displayed. At 2.38 eV, where the PL intensity shows a drop, the decay appears faster, as evidenced by the accumulation of isolines in the low intensity range.

Based on the PLE pattern, an interesting comparison can be made among PL spectra excited at energies resonant with Er^{3+} transitions (e.g., at 2.38 and 3.27 eV) and spectra obtained exciting within the nanophase excitation band at energies above 3.4 eV [Fig. 4(a)]. The erbium emission at 2.25 eV is narrow and structured when it is excited within the nanoclusters excitation band (spectrum excited at 3.70 eV). Compared with the same emission excited at other energies [2.4 and 3.27 eV in Fig. 4(a)], its shape suggests that the responsible sites are characterized by a more ordered environment. In fact, spectra excited at 3.27 eV ($^4I_{15/2} \rightarrow {}^4G_{11/2}$ transition) and 2.38 eV ($^4I_{15/2} \rightarrow {}^2H_{11/2}$ transition) show the typical broadened features of intracenter excited Er^{3+} ions in a glassy host. Figure 4(b) shows PL spectra in

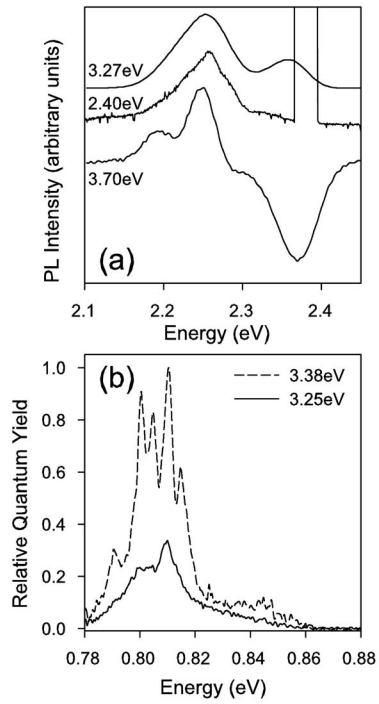

FIG. 4. (a) PL spectra (curves, left axis) excited at the indicated energies of 1 mol % Er, 8 mol % SnO_2:SiO_2. (b) Normalized absorbed and/or emitted photons ratio at the IR $^4I_{13/2} \rightarrow {}^4I_{15/2}$ transition for two excitation energies.

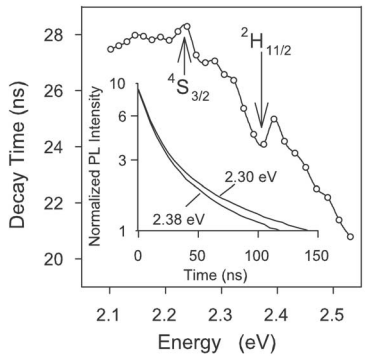

FIG. 5. Effective time decay constant from time resolved PL measurements as a function of the emission energy. Inset, representative PL decay curves at two emission energies.

the infrared region, corresponding to the $^4I_{13/2} \rightarrow {}^4I_{15/2}$ electronic transition of erbium, excited at two energies: 3.40 eV, inside the tail of the SnO_2 absorption edge, and 3.25 eV, corresponding to the $^4I_{15/2} \rightarrow {}^4G_{11/2}$ transition of erbium. These spectra, collected in identical conditions of light detection geometry and corrected for the absorption coefficient and excitation intensity at the two energies, are reported in units proportional to the ratio between the numbers of absorbed and emitted photons, allowing to compare the emission efficiency at the two excitation energies. Similar to Fig. 4(a), we note a change of shape and line narrowing when the excitation lies within the tail of the SnO_2 absorption edge. Moreover, the efficiency of the process is enhanced with respect to intracenter excitation.

These results indicate that a fraction of the erbium population is embedded in a crystalline surrounding, and only this fraction contributes significantly to the erbium luminescence when nanocrystals are excited. In fact, the observation of an unstructured emission spectrum excited at 2.38 eV [Fig. 4(a)] indicates that the structured erbium emission excited at 3.70 eV cannot be caused by absorption by erbium ions of 2.38 eV photons emitted by nanoclusters. In other words, a nonradiative pathway arising from excitation of nanoclusters populates the $^2H_{11/2}$ state of the Er^{3+} ions through an energy-transfer process from cluster to erbium.

Figure 5 shows the results and the analysis of time resolved measurements that further support the occurrence of a cluster-to-erbium energy-transfer process. Values of decay time τ are estimated from the experimental decay curves (see inset) at different emission energies. The decay curves are not single exponential functions. The reported data, determined from the time at $1/e$ reduction of the PL signal, are thus effective decay-time values. The spectral dependence of τ throughout the emission band shows faster decays in the high energy side of the emission energy range with respect to the low energy side of the band. This dependence reflects the higher probability of excitation migration from the high energy states within the ensemble of excited localized states responsible for the nanocluster light emission, with a resulting shortening of the decay time with respect to the low lying emitting levels.[16] The increase of τ at 2.25 eV is due to the slow emission of erbium from the $^4S_{3/2}$ state. A narrow abrupt decrease of τ instead accompanies the PL intensity lowering at 2.38 eV [see Fig. 4(a)], resonant with the $^4I_{15/2} \rightarrow {}^2H_{11/2}$ erbium transition. This clearly indicates an additional decay pathway that indeed is the energy-transfer process from nanoclusters to erbium ions suggested by the comparison of spectra in Fig. 4.

A quantitative estimation of the efficiency η of the energy transfer between the luminescent defect site of the nanoparticle and the nearby Er^{3+} ion (respectively, the donor and acceptor species in the energy-transfer process at 2.38 eV) can be made from the data in Fig. 2(b). The efficiency η can in fact be evaluated using the relation[16] $\eta = 1 - (I_{ET}/I_0)$ where I_{ET} is the PL intensity reduced by energy-transfer mechanisms and I_0 is the value expected in the absence of energy transfer [dashed spectrum in Fig. 2(b)]. From Fig. 2(b), the experimental intensity lowering $(I_0 - I_{exp})/I_0$ at 2.38 eV is about 70%. Since self-absorption by the material and energy-transfer effects concur to the lowering, an estimation of I_{ET} requires the evaluation of the absorption effects. This evaluation must take into account the experimental excitation and/or detection geometry (approximately antireflection) and the absorption coefficient at the excitation and emission energies. The expected PL intensity I_{SA} after reduction by self-absorption is approximately given by $I_0[1 - \exp(-\alpha_{Er}L)]$, where α_{Er} is the absorption coefficient at 2.38 eV and L is the effective optical path across the sample. Based on the absorption spectra in Fig. 2(a), only a $50\% \pm 5\%$ of PL turns out to be self-absorbed by the material, whereas the relative intensity I_{ET}/I_0 in the presence of energy transfer is about $80\% \pm 5\%$, pointing to an energy transfer yield η between excited donor and emitting acceptor of $20\% \pm 5\%$. The efficiency of excitation transfer from the whole ensemble of nanoclusters to the population of erbium ions is smaller since we must consider the following factors: (i) Not all the excited localized states of the nanoclusters are resonant with the 2.38 eV transition of erbium; thus, to account for this, the efficiency η must be scaled by the ratio Σ between resonant and out-of-resonance donor sites. This factor is estimated 6×10^{-2} from the superposition integral between the absorption band of erbium and the broad defect-related emission band of nanoclusters; (ii) a major fraction of Er^{3+} ions is dispersed in the glass and does not take part directly in the energy-transfer mechanism even though, due to the large erbium concentration, Er-Er dipole interactions may partially spread the excitation to the whole Er^{3+} population. On the other hand, only one erbium per nanocluster can be excited. As a result, the nanocluster concentration determines the upper limit of the number of Er^{3+} ions involved in the transfer process. The concentration of nanoclusters, known as the content of tin dioxide and the average cluster size resulting from TEM analysis, is about 2×10^{18} cm^{-3}, to be compared with the erbium concentration 2.25×10^{20} cm^{-3}. Therefore, the fraction ρ of Er^{3+} ions participating in the transfer process is only 1% in the investigated material. This result clearly calls for an optimization of the material in view of possible applications. Nevertheless, looking at the data in Fig. 4(a), the result evidences a much larger emission quantum yield of erbium excited by energy transfer in ordered environment with respect to erbium in the amorphous matrix. In fact, although the energy-transfer efficiency η is only

20%, further decreased by the estimated factors Σ and ρ, the 2.25 eV structured emission is the dominant erbium contribution of the PL spectrum excited within the SnO_2 gap. By contrast, 50% of nanocluster-emitted photons are self-absorbed without any evident broadened unstructured contribution due to emission of erbium embedded in the glass. A large quantum yield of the erbium ions near the nanoclusters is indeed confirmed by the spectra in Fig. 4(b) showing that energy transfer gives rise to PL about a factor 3 more intense than that excited by direct intracenter transitions.

In summary, the spectral and time resolved analysis of erbium photoluminescence demonstrates that SnO_2 nanocrystals can really activate energy-transfer mechanisms in silica. The wide-band-gap crystalline phase provides erbium with an excitation path starting from decay transitions of localized centers at the nanoclusters, and involving light emitting ions with an environment clearly reflecting the crystalline features of the nanostructures.

This work is supported in part by Italian Government (PRIN Project). One of the authors (S.B.) acknowledges support from the Fondazione Silvio Tronchetti Provera.

*Electronic address: sergio.brovelli@mater.unimib.it

[1] F. Priolo, G. Franz, D. Pacifici, and V. Vinciguerra, J. Appl. Phys. **89**, 264 (2001).

[2] M. Wojdak, M. Klik, M. Forcales, O. B. Gusev, T. Gregorkiewicz, D. Pacifici, G. Franzo, F. Priolo, and F. Iacona, Phys. Rev. B **69**, 233315 (2004).

[3] X. L. Wu, Y. F. Mei, G. G. Siu, K. L. Wong, K. Moulding, M. J. Stokes, C. L. Fu, and X. M. Bao, Phys. Rev. Lett. **86**, 3000 (2001).

[4] L. Eldada, Rev. Sci. Instrum. **75**, 575 (2004).

[5] M. R. Poulsen, P. I. Borel, J. Fage-Pedersen, J. Hubner, M. Kristensen, J. H. Povlsen, K. Rottwitt, M. Svalgaard, and W. Svendsen, Opt. Eng. **43**, 2821 (2003).

[6] W. J. Miniscalco, J. Lightwave Technol. **9**, 234 (1991).

[7] E. Desurvire, *Erbium-Doped Fiber Amplifiers—Principles and Applications* (Wiley, New York, 1994).

[8] N. Chiodini, A. Paleari, D. Di Martino, and G. Spinolo, Appl. Phys. Lett. **81**, 1702 (2002).

[9] N. Chiodini, F. Meinardi, F. Morazzoni, J. Padovani, A. Paleari, R. Scotti, and G. Spinolo, J. Mater. Chem. **11**, 926 (2001).

[10] E. J. H. Lee, C. Ribeiro, T. R. Giraldi, E. Longo, E. R. Leite, and J. A. Varela, Appl. Phys. Lett. **84**, 1745 (2004).

[11] N. Chiodini, A. Paleari, and G. Spinolo, Phys. Rev. Lett. **90**, 055507 (2003).

[12] N. Chiodini, A. Paleari, G. Spinolo, and P. J. Crespi, J. Non-Cryst. Solids **322**, 266 (2003).

[13] N. Chiodini, A. Paleari, G. Brambilla, and E. R. Taylor, Appl. Phys. Lett. **80**, 4449 (2002).

[14] A. C. Yanes, J. D. Castillo, M. Torres, J. Peraza, V. D. Rodríguez, and J. Méndez-Ramos, Appl. Phys. Lett. **85**, 2343 (2002).

[15] M. Nogami, T. Enomoto, and T. Hayakawa, J. Lumin. **97**, 147 (2002).

[16] J. R. Lakowicz, *Principles of Fluorescence Spectroscopy* (Kluwer Academic/Plenum, New York, 1999).